

A NEW METHOD FOR THE DATA COMPLETION PROBLEM AND APPLICATION TO OBSTACLE DETECTION

FABIEN CAUBET*, MARC DAMBRINE†, AND HELMUT HARBRECHT‡

Abstract. The present article is devoted to the study of two well-known inverse problems, that is the data completion problem and the inverse obstacle problem. The general idea is to reconstruct some boundary conditions and/or to identify an obstacle or void of different conductivity which is contained in a domain, from measurements of voltage and currents on the outer boundary of the domain. We focus here on Laplace's equation.

Firstly, we use a penalized Kohn-Vogelius functional in order to numerically solve the data completion problem, which consists in recovering some boundary conditions from partial Cauchy data. The functional to be minimized is quadratic, hence we compute its minimum by solving the linearized equation. Secondly, we propose to build an iterative method for the inverse obstacle problem based on the combination of the previously mentioned data completion subproblem and the so-called *trial method*. The underlying boundary value problems are efficiently computed by means of boundary integral equations and several numerical simulations show the applicability and feasibility of our new approach. For the numerical simulations, we focus on star-shaped domains in the two dimensional case.

Key words. Cauchy problem, Data completion problem, Inverse obstacle problem, Laplace's equation, Kohn-Vogelius functional.

AMS subject classifications. 35R30, 35R25, 35N25, 49M15.

1. Introduction. We deal in this article with the inverse obstacle problem which is defined as follows. Let Ω be a bounded connected Lipschitz open set of \mathbb{R}^d , where $d = 2$ or $d = 3$, with a boundary $\partial\Omega$. For some nontrivial Cauchy data $(f_m, g_m) \in H^{1/2}(\partial\Omega) \times H^{-1/2}(\partial\Omega)$ on the outer boundary, which corresponds to a pair of current/voltage measurements, we consider the following inverse problem:

$$(1.1) \quad \begin{array}{l} \text{Find a set } \omega^* \in \mathcal{D} \text{ and a solution } u \in H^1(\Omega \setminus \overline{\omega^*}) \\ \text{of the following overdetermined boundary value problem:} \\ \left\{ \begin{array}{ll} \Delta u = 0 & \text{in } \Omega \setminus \overline{\omega^*}, \\ u = f_m & \text{on } \partial\Omega, \\ \partial_{\mathbf{n}} u = g_m & \text{on } \partial\Omega, \\ u = 0 & \text{on } \partial\omega^*, \end{array} \right. \end{array}$$

where $\mathcal{D} = \{\omega \Subset \Omega, \partial\omega \text{ is Lipschitz and } \Omega \setminus \overline{\omega} \text{ is connected}\}$ and \mathbf{n} is the outer unit normal to $\Omega \setminus \overline{\omega}$. In other words, we want to detect an inclusion ω^* characterized by a homogeneous Dirichlet boundary condition from the knowledge of the Dirichlet and Neumann boundary conditions on the exterior boundary $\partial\Omega$. Notice that a only a single pair of Cauchy data is used.

Then the problem under consideration is a special case (assuming a constant conductivity with a void of connected complement) of the general conductivity reconstruction problem also called Electrical Impedance Tomography (EIT). EIT is used in medical imaging to reconstruct the electric conductivity of a part of the body from

*Institut de Mathématiques de Toulouse, Université de Toulouse, 31062 Toulouse Cedex 9, France. fabien.caubet@math.univ-toulouse.fr

†Laboratoire de Mathématiques et de leurs Applications, Université de Pau et des Pays de l'Adour, 64000 Pau, France. marc.dambrine@univ-pau.fr

‡Departement Mathematik und Informatik, Universität Basel, Spiegelgasse 1, 4051 Basel, Switzerland. helmut.harbrecht@unibas.ch

measurements of currents and voltages at the surface (see, e.g., [37]). The same technique is also used in geophysical explorations. An important special case consists in reconstructing the shape of an unknown inclusion or void assuming a constant conductivity. Notice that the continuum model is not a realistic model for EIT and more realistic electrode models exist (see [28, 29, 25, 36]). However we focus in this paper on this continuum model.

It is known that problem (1.1) admits at most one solution, as claimed by the following *identifiability result* (see, e.g., [10, Theorem 1.1] or [19, Theorem 5.1]).

THEOREM 1.1. *The domain ω and the function u which is assumed to be continuous up to the boundaries that satisfy (1.1) are uniquely defined by the nontrivial Cauchy data (f_m, g_m) .*

It is also well-known that problem (1.1) is severely ill-posed: the problem may fail to have a solution and, even when a solution exists, the problem is highly unstable (see, e.g., [4, 20]).

This inverse problem has been intensively investigated by numerous methods. We can cite for example sampling methods [38], methods based on conformal mappings [2, 27], on integral equations [35, 40], methods using the full Dirichlet-to-Neumann map at the outer boundary [11, 12], or level-set methods coupled with quasi-reversibility in the exterior approach [10]. We also refer for example to [17, 31] for numerical algorithms and to [5, 23] for particular results concerning uniqueness.

In [39], the problem under consideration has been reformulated as a shape optimization problem for the Kohn-Vogelius functional. Then, seeking the unknown inclusion is equivalent to seeking the minimizer of an energy functional. Much attention has been spent on the analysis of this approach (see, e.g., [3, 21]) and its comparison with a least-squares tracking type functionals. These kind of methods have some advantages such as being adaptable for several partial differential equations, such as the Stokes system (see, e.g., [13, 15, 26]), and for obstacles characterized by different boundary conditions, such as Neumann or generalized boundary conditions (see, e.g., [6, 14]).

In this article, we propose a new point of view to numerically solve this model inverse obstacle problem. We focus on the two-dimensional case and assume that the inclusion is star-shaped and perfectly conducting. Then, we build an iterative sequence of domains using the combination of a data completion subproblem and the so-called *trial method* which is used to control the evolution of the inclusion boundary. This means that, given an inclusion ω , we compute an harmonic function $u \in H^1(\Omega \setminus \bar{\omega})$ which admits the Cauchy data (f_m, g_m) at the outer boundary $\partial\Omega$. With the help of the Cauchy data at the interior boundary $\partial\omega$, we aim at updating the interior boundary such that the desired Dirichlet condition $u = 0$ holds at the new interior boundary. The data completion problem is solved by minimizing a Kohn-Vogelius functional thanks to the resolution of a regularized linearized equation, which is efficient since the functional is quadratic.

Organization of the article. The rest of the article is organized as follows. In Section 2, we introduce the data completion problem which we intend to solve by means of the minimization of a Kohn-Vogelius functional, also introduced in this section. We additionally provide all the general notations and assumptions used throughout the article. In Section 3, we provide some properties concerning the considered boundary value problems and compute the gradient and the Hessian of the

Kohn-Vogelius functional. Then, in Section 4, we introduce the Tikhonov regularization term needed to numerically minimize the functional. The minimization of this regularized functional is considered by means of a Newton scheme. Especially, numerical results are presented, which demonstrate that our approach yields an efficient solution of the data completion problem. In Section 5, we focus on the numerical resolution of the inverse obstacle problem. To this end, we present the so-called *trial method*, used to update an approximated inclusion's boundary from the information obtained from the previous data completion step. Numerical results validate that the proposed approach is feasible to reconstruct inclusions in the inverse obstacle problem at least on a model case a single star-shapes inclusion. Finally, in Section 6, we state concluding remarks.

2. Introduction of general notations and of the considered problems.

2.1. Introduction of the general notations. For a bounded open set Ω of \mathbb{R}^d ($d \in \mathbb{N} \setminus \{0\}$) with a (piecewise) Lipschitz boundary $\partial\Omega$, we precise that the notation $\int_{\Omega} u$ means $\int_{\Omega} u(\mathbf{x})d\mathbf{x}$ which is the classical Lebesgue integral. Moreover we use the notation $\int_{\partial\Omega} u$ to denote the boundary integral $\int_{\partial\Omega} u(\mathbf{x})ds(\mathbf{x})$, where ds represents the surface Lebesgue measure on the boundary. We also introduce the exterior unit normal \mathbf{n} of the domain Ω and $\partial_{\mathbf{n}}u$ will denote the normal derivative of u .

We denote by $L^2(\Omega)$, $L^2(\partial\Omega)$, $H^1(\Omega)$, $H^1(\partial\Omega)$, the usual Lebesgue and Sobolev spaces of scalar functions in Ω or on $\partial\Omega$. The classical norm and semi-norm on $H^1(\Omega)$ are respectively denoted by $\|\cdot\|_{H^1}$ and $|\cdot|_{H^1}$. Moreover $\langle \cdot, \cdot \rangle$ denotes the following product, for all $u, v \in H^1(\Omega)$,

$$\langle u, v \rangle := \int_{\Omega} \nabla u \cdot \nabla v \quad \text{so that} \quad |u|_{H^1(\Omega)}^2 = \langle u, u \rangle.$$

2.2. Introduction of the data completion problem. We recall that we consider in this article a bounded connected Lipschitz open set Ω of \mathbb{R}^d ($d = 2$ or $d = 3$) and an inclusion $\omega \in \mathcal{D}$, with $\mathcal{D} = \{\omega \in \Omega, \partial\omega \text{ is Lipschitz and } \Omega \setminus \bar{\omega} \text{ is connected}\}$. Let us consider some nontrivial Cauchy data $(f_m, g_m) \in H^{1/2}(\partial\Omega) \times H^{-1/2}(\partial\Omega)$.

The data completion problem consists in recovering data on $\partial\omega$, from the overdetermined data (f_m, g_m) on $\partial\Omega$, that is:

$$(2.1) \quad \begin{cases} \text{Find } u \in H^1(\Omega \setminus \bar{\omega}) \text{ such that} \\ \Delta u = 0 & \text{in } \Omega \setminus \bar{\omega}, \\ u = f_m & \text{on } \partial\Omega, \\ \partial_{\mathbf{n}}u = g_m & \text{on } \partial\Omega. \end{cases}$$

Of course, the previous problem is not standard. In general, it admits only a local solution (that is defined in the neighborhood of $\partial\Omega$ under regularity assumptions) by the Cauchy-Kowalevskaya theorem. Since we are interested in global solutions, this result is not satisfactory and we have to define the notion of *compatible data*.

DEFINITION 2.1. A pair $(f_m, g_m) \in H^{1/2}(\partial\Omega) \times H^{-1/2}(\partial\Omega)$ is said **compatible** if the Cauchy problem (2.1) has a (necessarily unique) solution.

When data is compatible, the unknown u is uniquely determined by either its Dirichlet trace or its Neumann trace on the inner boundary $\partial\omega$. The property of being compatible is not open: indeed the set of compatible couples is dense in

$H^{1/2}(\partial\Omega) \times H^{-1/2}(\partial\Omega)$. Hence, if a given pair (f_m, g_m) is not compatible, we may approximate it by a sequence of compatible data. Typical density results have been stated by Andrieux *et al.* in [1, Lemma 2.1] or Fursikov in [24], where the following result is given.

LEMMA 2.2. *We have the two following density results.*

1. *For a fixed $f_m \in H^{1/2}(\partial\Omega)$, the set of compatible data g is dense in $H^{-1/2}(\partial\Omega)$.*
2. *For a fixed $g_m \in H^{-1/2}(\partial\Omega)$, the set of compatible f is dense in $H^{1/2}(\partial\Omega)$.*

Therefore, any numerical scheme should incorporate a regularization step. Several approaches have been considered to solve the data completion problem. Among others, we mention the works of Kozlov *et al.* [33], Cimetière *et al.* [18], Ben Belgacem *et al.* [7, 8].

We shall follow the energy based strategy introduced by Andrieux *et al.* in [1] by the minimization of the Kohn-Vogelius like functional which admits the solution of problem (2.1) as minimizer, if such a solution exists. Notice that such a functional turns to be quadratic and convex. Surprisingly, to the best of our knowledge, only gradient based numerical schemes have been studied for the resolution of this problem. We will describe in this article the Newton method that is completely suited for quadratic objectives.

In order to deal with the ill-posedness previously mentioned, we consider a Tikhonov regularization of the functional which ensures the existence of a minimizer even for not compatible data thanks to the gained of coerciveness and, in case of compatible data, the convergence towards the exact solution (see, e.g., [16, Proposition 2.5 and Theorem 2.6]).

2.3. The Kohn-Vogelius functional. As previously mentioned, the data completion problem (2.1) can be studied through the minimization of a Kohn-Vogelius cost functional (see [32]). To this end, we introduce the two maps \mathbf{u}_{DN} and \mathbf{u}_{ND} defined as follows

$$(2.2) \quad \begin{aligned} \mathbf{u}_{\text{DN}} &: H^{1/2}(\partial\Omega) \times H^{-1/2}(\partial\omega) \longrightarrow H^1(\Omega \setminus \bar{\omega}), \\ \mathbf{u}_{\text{ND}} &: H^{-1/2}(\partial\Omega) \times H^{1/2}(\partial\omega) \longrightarrow H^1(\Omega \setminus \bar{\omega}), \end{aligned}$$

where $\mathbf{u}_{\text{DN}}(f, \psi) \in H^1(\Omega \setminus \bar{\omega})$ solves the boundary values problem

$$(2.3) \quad \begin{cases} \Delta u = 0 & \text{in } \Omega \setminus \bar{\omega}, \\ u = f & \text{on } \partial\Omega, \\ \partial_{\mathbf{n}} u = \psi & \text{on } \partial\omega, \end{cases}$$

and where $\mathbf{u}_{\text{ND}}(g, \phi) \in H^1(\Omega \setminus \bar{\omega})$ solves the boundary values problem

$$(2.4) \quad \begin{cases} \Delta u = 0 & \text{in } \Omega \setminus \bar{\omega}, \\ \partial_{\mathbf{n}} u = g & \text{on } \partial\Omega, \\ u = \phi & \text{on } \partial\omega. \end{cases}$$

Notice that the indices mean the type of boundary condition, where the first one indicates the outer boundary and the second one the inner boundary.

To tackle the inverse problem, one tries to solve the problem:

$$\begin{aligned} \text{Find } (\phi, \psi) \in H^{1/2}(\partial\omega) \times H^{-1/2}(\partial\omega) \text{ such that} \\ \mathbf{u}_{\text{DN}}(f_m, \psi) = \mathbf{u}_{\text{ND}}(g_m, \phi). \end{aligned}$$

Thanks to the linearity of the maps \mathbf{u}_{ND} and \mathbf{u}_{DN} , this is equivalent to:

$$\begin{aligned} & \text{Find } (\phi, \psi) \in \text{H}^{1/2}(\partial\omega) \times \text{H}^{-1/2}(\partial\omega) \text{ such that} \\ & \mathbf{u}_{\text{DN}}(0, \psi) - \mathbf{u}_{\text{ND}}(0, \phi) = -(\mathbf{u}_{\text{DN}}(f_m, 0) - \mathbf{u}_{\text{ND}}(g_m, 0)). \end{aligned}$$

Notice that this is a standard linear inverse problem associated to the linear operator

$$\begin{aligned} \mathbf{A} : \text{H}^{1/2}(\partial\omega) \times \text{H}^{-1/2}(\partial\omega) &\longrightarrow \text{H}^1(\Omega \setminus \bar{\omega}) \\ (\phi, \psi) &\longmapsto \mathbf{u}_{\text{DN}}(0, \psi) - \mathbf{u}_{\text{ND}}(0, \phi). \end{aligned}$$

Of course, the right hand side $\mathbf{b} := -(\mathbf{u}_{\text{DN}}(f_m, 0) - \mathbf{u}_{\text{ND}}(g_m, 0))$ may belong or may not belong to the range $R(\mathbf{A})$ of \mathbf{A} , depending on the fact that data are compatible or not.

We try to solve the previous linear equation in a least squares meaning. We focus on the following optimization problem

$$(\phi^*, \psi^*) \in \underset{(\phi, \psi) \in \text{H}_0^{1/2}(\partial\omega) \times \text{H}^{-1/2}(\partial\omega)}{\text{argmin}} \mathcal{K}(\phi, \psi),$$

where $\mathcal{K} : \text{H}^{1/2}(\partial\omega) \times \text{H}^{-1/2}(\partial\omega) \rightarrow \mathbb{R}$ is the non-negative Kohn-Vogelius cost functional defined by

$$\mathcal{K}(\phi, \psi) := \frac{1}{2} |\mathbf{A}(\phi, \psi) - \mathbf{b}|_{\text{H}^1(\Omega \setminus \bar{\omega})}^2.$$

Notice that this criterion is quadratic as the square of a affine map and also writes

$$\begin{aligned} \mathcal{K}(\phi, \psi) &= \frac{1}{2} |\mathbf{u}_{\text{DN}}(f_m, \psi) - \mathbf{u}_{\text{ND}}(g_m, \phi)|_{\text{H}^1(\Omega \setminus \bar{\omega})}^2 \\ (2.5) \quad &= \frac{1}{2} \int_{\Omega \setminus \bar{\omega}} |\nabla \mathbf{u}_{\text{DN}}(f_m, \psi) - \nabla \mathbf{u}_{\text{ND}}(g_m, \phi)|^2. \end{aligned}$$

The connection between the original inverse problem and the minimization is given by next lemma.

LEMMA 2.3. *The inverse problem (2.1) has a solution if and only if the functional \mathcal{K} has a minimizer (ϕ, ψ) and $\mathcal{K}(\phi, \psi) = 0$. Notice that the minimizer is unique up to an additive constant: if $\mathcal{K}(\phi_1, \psi_1) = 0 = \mathcal{K}(\phi_2, \psi_2)$ then there is a constant c such that $\phi_1 = \phi_2 + c$ and $\psi_1 = \psi_2$.*

Proof. For a given and known inclusion ω , if the inverse problem (2.1) has a solution, then $\mathbf{u}_{\text{DN}}(f_m, \psi) = \mathbf{u}_{\text{ND}}(g_m, \phi)$ and $\mathcal{K}(\phi, \psi) = 0$. Conversely, if we assume that $\mathcal{K}(\phi, \psi) = 0$ then $\nabla \mathbf{u}_{\text{DN}}(f_m, \psi) = \nabla \mathbf{u}_{\text{ND}}(g_m, \phi)$ and there is a constant c such that $\mathbf{u}_{\text{DN}}(f_m, \psi) = \mathbf{u}_{\text{ND}}(g_m, \phi) + c = \mathbf{u}_{\text{ND}}(g_m, \phi + c)$. \square

The usual theory of linear inverse problems should be applied. That is, we solve the *normal equation* $\mathbf{A}^\top \mathbf{A}(\phi, \psi) = \mathbf{A}^\top \mathbf{b}$ or its *regularized version* $(\mathbf{A}^\top \mathbf{A} + \varepsilon \mathbf{B}^\top \mathbf{B})(\phi, \psi) = \mathbf{A}^\top \mathbf{b}$, where \mathbf{B} is a *regularization operator* and where $\varepsilon > 0$. However it involves the adjoint \mathbf{A}^\top of \mathbf{A} and hence to manipulate the scalar product in the space $\text{H}^{1/2}(\partial\omega) \times \text{H}^{-1/2}(\partial\omega)$.

The main difficulty of this approach is that the scalar product in the spaces $\text{H}^{1/2}(\partial\omega)$ and $\text{H}^{-1/2}(\partial\omega)$ is not tractable with from a practical point of view when one uses the optimize then discretize approach. On the converse, if one first discretizes the equations, and then computes the discrete adjoint, the usual theory can be applied. In

the following, we want to remain at the continuous level and reduce the minimization of the Kohn-Vogelius objective to such a linear inverse problem in a simple way thanks to the Newton point of view. Since the objective \mathcal{K} is quadratic, its hessian is constant and its minimizer can be computed by a single step in Newton method.

REMARK 2.4. *Note that the two problems (2.3) and (2.4) are well-posed for any given boundary conditions $(\phi, \psi) \in \mathbf{H}^{1/2}(\partial\omega) \times \mathbf{H}^{-1/2}(\partial\omega)$, without additional compatibility conditions between f_m and ψ for the first problem and between g_m and ϕ for the second. This is of particular interest for numerical implementations, as the considered setting allows to consider the classical Sobolev spaces and, therefore, the implementations can be done with classical finite element method softwares without any additional adjustments.*

3. Some properties concerning the data completion problem.

3.1. Properties of the maps \mathbf{u}_{DN} and \mathbf{u}_{ND} . Let us first emphasize some properties of the maps defined in (2.2) we should use.

PROPOSITION 3.1 (Properties of the boundary values problems). *We have the following statements.*

1. *The maps \mathbf{u}_{DN} and \mathbf{u}_{ND} are linear: for all $(f_1, \psi_1), (f_2, \psi_2) \in \mathbf{H}^{1/2}(\partial\Omega) \times \mathbf{H}^{-1/2}(\partial\omega)$, there holds*

$$\begin{aligned} \mathbf{u}_{\text{DN}}(f_1 + f_2, \psi_1 + \psi_2) &= \mathbf{u}_{\text{DN}}(f_1, \psi_1) + \mathbf{u}_{\text{DN}}(f_2, \psi_2) \\ &= \mathbf{u}_{\text{DN}}(f_2, \psi_1) + \mathbf{u}_{\text{DN}}(f_1, \psi_2) \end{aligned}$$

and

$$\begin{aligned} \mathbf{u}_{\text{ND}}(g_1 + g_2, \phi_1 + \phi_2) &= \mathbf{u}_{\text{ND}}(g_1, \phi_1) + \mathbf{u}_{\text{ND}}(g_2, \phi_2) \\ &= \mathbf{u}_{\text{ND}}(g_2, \phi_1) + \mathbf{u}_{\text{ND}}(g_1, \phi_2). \end{aligned}$$

2. *There are positive constants C_1 and C_2 such that*

$$(3.1) \quad \begin{aligned} C_1 \|\phi\|_{\mathbf{H}^{1/2}(\partial\omega)} &\leq \|\mathbf{u}_{\text{ND}}(0, \phi)\|_{\mathbf{H}^1(\Omega \setminus \bar{\omega})} \leq C_2 \|\phi\|_{\mathbf{H}^{1/2}(\partial\omega)}, \\ C_1 \|\psi\|_{\mathbf{H}^{-1/2}(\partial\omega)} &\leq \|\mathbf{u}_{\text{DN}}(0, \psi)\|_{\mathbf{H}^1(\Omega \setminus \bar{\omega})} \leq C_2 \|\psi\|_{\mathbf{H}^{-1/2}(\partial\omega)}, \end{aligned}$$

for all $(\phi, \psi) \in \mathbf{H}^{1/2}(\partial\omega) \times \mathbf{H}^{-1/2}(\partial\omega)$.

3. *There holds*

$$\begin{aligned} \langle \mathbf{u}_{\text{DN}}(f_1, \psi_1), \mathbf{u}_{\text{DN}}(f_2, \psi_2) \rangle &= \int_{\partial\Omega} f_1 \partial_{\mathbf{n}} \mathbf{u}_{\text{DN}}(f_2, \psi_2) + \int_{\partial\omega} \mathbf{u}_{\text{DN}}(f_1, \psi_1) \psi_2 \\ &= \int_{\partial\Omega} f_2 \partial_{\mathbf{n}} \mathbf{u}_{\text{DN}}(f_1, \psi_1) + \int_{\partial\omega} \mathbf{u}_{\text{DN}}(f_2, \psi_2) \psi_1, \\ \langle \mathbf{u}_{\text{DN}}(f_1, \psi_1), \mathbf{u}_{\text{ND}}(g_1, \phi_1) \rangle &= \int_{\partial\Omega} f_1 g_1 + \int_{\partial\omega} \mathbf{u}_{\text{DN}}(f_1, \psi_1) \partial_{\mathbf{n}} \mathbf{u}_{\text{ND}}(g_1, \phi_1) \\ &= \int_{\partial\Omega} \mathbf{u}_{\text{ND}}(g_1, \phi_1) \partial_{\mathbf{n}} \mathbf{u}_{\text{DN}}(f_1, \psi_1) + \int_{\partial\omega} \phi_1 \psi_1, \\ \langle \mathbf{u}_{\text{ND}}(g_1, \phi_1), \mathbf{u}_{\text{ND}}(g_2, \phi_2) \rangle &= \int_{\partial\Omega} \mathbf{u}_{\text{ND}}(g_1, \phi_1) g_2 + \int_{\partial\omega} \phi_1 \partial_{\mathbf{n}} \mathbf{u}_{\text{ND}}(g_2, \phi_2) \\ &= \int_{\partial\Omega} \mathbf{u}_{\text{ND}}(g_2, \phi_2) g_1 + \int_{\partial\omega} \phi_2 \partial_{\mathbf{n}} \mathbf{u}_{\text{ND}}(g_1, \phi_1), \end{aligned}$$

for all $(f_1, \psi_1), (f_2, \psi_2) \in \mathbf{H}^{1/2}(\partial\Omega) \times \mathbf{H}^{-1/2}(\partial\omega)$ and all $(g_1, \phi_1), (g_2, \phi_2) \in \mathbf{H}^{-1/2}(\partial\Omega) \times \mathbf{H}^{1/2}(\partial\omega)$.

Proof. The first assertion is a trivial consequence of the superposition principle. Let us prove the point $C_1 \|\psi\|_{H^{-1/2}(\partial\omega)} \leq \|\mathbf{u}_{\text{DN}}(0, \psi)\|_{H^1(\Omega \setminus \bar{\omega})}$. By definition of the dual norm,

$$\begin{aligned} \|\psi\|_{H^{-1/2}(\partial\omega)} &= \sup_{\|\phi\|_{H^{1/2}(\partial\omega)}=1} \langle \phi, \psi \rangle_{H^{1/2}(\partial\omega) \times H^{-1/2}(\partial\omega)} \\ &= \int_{\partial\omega} \partial_{\mathbf{n}} \mathbf{u}_{\text{DN}}(0, \psi) \Phi = \int_{\Omega \setminus \bar{\omega}} \nabla \mathbf{u}_{\text{DN}}(0, \psi) \cdot \nabla \Phi, \end{aligned}$$

where $\Phi \in H^1(\Omega \setminus \bar{\omega})$ is the harmonic extension of ϕ so that it holds

$$\|\Phi\|_{H^1(\Omega \setminus \bar{\omega})} = \|\phi\|_{H^{1/2}(\partial\omega)} = 1.$$

We conclude that

$$\|\psi\|_{H^{-1/2}(\partial\omega)} \leq \|\mathbf{u}_{\text{DN}}(0, \psi)\|_{H^1(\Omega \setminus \bar{\omega})} \|\Phi\|_{H^1(\Omega \setminus \bar{\omega})} = \|\mathbf{u}_{\text{DN}}(0, \psi)\|_{H^1(\Omega \setminus \bar{\omega})}.$$

The others inequalities of the second second assertion comes from usual a priori elliptic estimate. The third assertion is a consequence of the Green formulae. \square

Let us remark that the third assertion of Proposition 3.1 implies in particular the following formulae which is useful to transform an integral over the outer boundary into an integral over the inner boundary:

$$\begin{aligned} \langle \mathbf{u}_{\text{DN}}(0, \psi), \mathbf{u}_{\text{DN}}(f, 0) \rangle &= 0 = \int_{\partial\Omega} f \partial_{\mathbf{n}} \mathbf{u}_{\text{DN}}(0, \psi) + \int_{\partial\omega} \mathbf{u}_{\text{DN}}(f, 0) \psi, \\ \int_{\partial\Omega} \mathbf{u}_{\text{ND}}(0, \phi) \partial_{\mathbf{n}} \mathbf{u}_{\text{DN}}(f, 0) &= \int_{\partial\omega} \mathbf{u}_{\text{DN}}(f, 0) \partial_{\mathbf{n}} \mathbf{u}_{\text{ND}}(0, \phi), \\ \langle \mathbf{u}_{\text{ND}}(g, 0), \mathbf{u}_{\text{ND}}(0, \phi) \rangle &= 0 = \int_{\partial\Omega} \mathbf{u}_{\text{ND}}(0, \phi) g + \int_{\partial\omega} \phi \partial_{\mathbf{n}} \mathbf{u}_{\text{ND}}(g, 0). \end{aligned}$$

Another consequence of these integration by parts formulae is the following alternative expression of the Kohn-Vogelius objective:

$$(3.2) \quad \begin{aligned} \mathcal{K}(\phi, \psi) &= \int_{\partial\Omega} (f_{\text{m}} - \mathbf{u}_{\text{ND}}(g_{\text{m}}, \phi)) (\partial_{\mathbf{n}} \mathbf{u}_{\text{DN}}(f_{\text{m}}, \psi) - g_{\text{m}}) \\ &\quad + \int_{\partial\omega} (\mathbf{u}_{\text{DN}}(f_{\text{m}}, \psi) - \phi) (\psi - \partial_{\mathbf{n}} \mathbf{u}_{\text{ND}}(g_{\text{m}}, \phi)). \end{aligned}$$

REMARK 3.2. *Let us emphasize that we use the usual abusive notation since the boundary integrals are to be understood as duality product between a Dirichlet trace in $H^{1/2}$ and a Neumann trace in $H^{-1/2}$.*

3.2. Properties of the Kohn-Vogelius objective \mathcal{K} . The main properties of the functional defined by (2.5) can be summarized as follow.

PROPOSITION 3.3 (Properties of the Kohn-Vogelius objective). *We have the following statements.*

1. *The functional \mathcal{K} is convex, positive and*

$$\inf \left\{ \mathcal{K}(\phi, \psi); (\phi, \psi) \in H^{1/2}(\partial\omega) \times H^{-1/2}(\partial\omega) \right\} = 0.$$

2. *The functional \mathcal{K} is quadratic with gradient*

$$\begin{aligned} D\mathcal{K}(\phi, \psi) \cdot [\delta\phi, \delta\psi] &= \int_{\partial\omega} [\partial_{\mathbf{n}}\mathbf{u}_{\text{ND}}(\partial_{\mathbf{n}}\mathbf{u}_{\text{DN}}(f_{\text{m}}, \psi), \phi) - \psi] \delta\phi \\ &\quad + [\mathbf{u}_{\text{DN}}(\mathbf{u}_{\text{ND}}(g_{\text{m}}, \phi), \psi) - \phi] \delta\psi, \end{aligned}$$

and constant Hessian

$$\begin{aligned} D^2\mathcal{K}(\phi, \psi) \cdot ([\delta\phi_1, \delta\psi_1], [\delta\phi_2, \delta\psi_2]) \\ = \langle \mathbf{u}_{\text{DN}}(0, \delta\psi_1) - \mathbf{u}_{\text{ND}}(0, \delta\phi_1), \mathbf{u}_{\text{DN}}(0, \delta\psi_2) - \mathbf{u}_{\text{ND}}(0, \delta\phi_2) \rangle. \end{aligned}$$

The first point of this statement is proved in [16, Proposition 2.2] but we recall the proof for reader's convenience.

Proof. We prove each statement.

1. Convexity and positiveness are obvious. To prove that $\inf_{(\phi, \psi)} \mathcal{K}(\phi, \psi) = 0$, we have to consider two cases. If the pair $(f_{\text{m}}, g_{\text{m}})$ is compatible, we consider the solution u_{ex} of the Cauchy problem (2.1) and we define $\phi^* := u_{ex}|_{\partial\omega}$ and $\psi^* := \partial_{\mathbf{n}}u_{ex}|_{\partial\omega}$ and then obtain $\mathcal{K}(\phi^*, \psi^*) = 0$. Let us now focus on the non-compatible case. Thanks to the density lemma 2.2, we can approximate f_{m} by a sequence $(f_{\text{m}}^n)_n$ in a way that the pairs $(f_{\text{m}}^n, g_{\text{m}})_n$ are compatibles for all $n \in \mathbb{N}$. For each n , consider (ϕ_n^*, ψ_n^*) to be the minimizer of the Kohn-Vogelius function for the data $(f_{\text{m}}^n, g_{\text{m}})$ which implies that $\nabla\mathbf{u}_{\text{DN}}(f_{\text{m}}^n, \psi_n^*) = \nabla\mathbf{u}_{\text{ND}}(g_{\text{m}}, \phi_n^*)$. Then, we have

$$\begin{aligned} \mathcal{K}(\phi_n^*, \psi_n^*) &= \frac{1}{2} |\mathbf{u}_{\text{DN}}(f_{\text{m}}, \psi_n^*) - \mathbf{u}_{\text{DN}}(g_{\text{m}}, \phi_n^*)|_{\text{H}^1(\Omega \setminus \bar{\omega})}^2 \\ &= \frac{1}{2} |\mathbf{u}_{\text{DN}}(f_{\text{m}}, \psi_n^*) - \mathbf{u}_{\text{DN}}(f_{\text{m}}^n, \psi_n^*)|_{\text{H}^1(\Omega \setminus \bar{\omega})}^2 \\ &= \frac{1}{2} |\mathbf{u}_{\text{DN}}(f_{\text{m}} - f_{\text{m}}^n, 0)|_{\text{H}^1(\Omega \setminus \bar{\omega})}^2 \\ &\leq C \|f_{\text{m}} - f_{\text{m}}^n\|_{\text{H}^{1/2}(\partial\Omega)}^2 \xrightarrow{n \rightarrow \infty} 0, \end{aligned}$$

which concludes the proof.

2. An elementary computation shows that

$$\begin{aligned} \mathcal{K}(\phi + \delta\phi, \psi + \delta\psi) \\ &= \frac{1}{2} |\mathbf{u}_{\text{DN}}(f_{\text{m}}, \psi) - \mathbf{u}_{\text{ND}}(g_{\text{m}}, \phi) + \mathbf{u}_{\text{DN}}(0, \delta\psi) - \mathbf{u}_{\text{ND}}(0, \delta\phi)|_{\text{H}^1(\Omega \setminus \bar{\omega})}^2 \\ &= \mathcal{K}(\phi, \psi) + \langle \mathbf{u}_{\text{DN}}(f_{\text{m}}, \psi) - \mathbf{u}_{\text{ND}}(g_{\text{m}}, \phi), \mathbf{u}_{\text{DN}}(0, \delta\psi) - \mathbf{u}_{\text{ND}}(0, \delta\phi) \rangle \\ &\quad + \frac{1}{2} |\mathbf{u}_{\text{DN}}(0, \delta\psi) - \mathbf{u}_{\text{ND}}(0, \delta\phi)|_{\text{H}^1(\Omega \setminus \bar{\omega})}^2 \end{aligned}$$

We identify the linear and quadratic terms in this expression (that are continuous thanks to (3.1)) and obtain a first expression of its derivatives

$$\begin{aligned} D\mathcal{K}(\phi, \psi) \cdot [\delta\phi, \delta\psi] \\ = \langle \mathbf{u}_{\text{DN}}(f_{\text{m}}, \psi) - \mathbf{u}_{\text{ND}}(g_{\text{m}}, \phi), \mathbf{u}_{\text{DN}}(0, \delta\psi) - \mathbf{u}_{\text{ND}}(0, \delta\phi) \rangle \end{aligned}$$

and the quadratic form

$$D^2\mathcal{K}(\phi, \psi) \cdot ([\delta\phi, \delta\psi], [\delta\phi, \delta\psi]) = |\mathbf{u}_{\text{DN}}(0, \delta\psi) - \mathbf{u}_{\text{ND}}(0, \delta\phi)|_{\text{H}^1(\Omega \setminus \bar{\omega})}^2,$$

and finally by polarity

$$\begin{aligned} D^2\mathcal{K}(\phi, \psi) \cdot ([\delta\phi_1, \delta\psi_1], [\delta\phi_2, \delta\psi_2]) \\ = \langle \mathbf{u}_{\text{DN}}(0, \delta\psi_1) - \mathbf{u}_{\text{ND}}(0, \delta\phi_1), \mathbf{u}_{\text{DN}}(0, \delta\psi_2) - \mathbf{u}_{\text{ND}}(0, \delta\phi_2) \rangle. \end{aligned}$$

However, this writing is not directly useful since the dependency in $(\delta\phi, \delta\psi)$ is not completely explicit. We therefore expand the expression of the gradient

$$\begin{aligned} D\mathcal{K}(\phi, \psi) \cdot [\delta\phi, \delta\psi] &= \langle \mathbf{u}_{\text{DN}}(f_m, \psi), \mathbf{u}_{\text{DN}}(0, \delta\psi) \rangle - \langle \mathbf{u}_{\text{DN}}(f_m, \psi), \mathbf{u}_{\text{ND}}(0, \delta\phi) \rangle \\ &\quad - \langle \mathbf{u}_{\text{ND}}(g_m, \phi), \mathbf{u}_{\text{DN}}(0, \delta\psi) \rangle + \langle \mathbf{u}_{\text{ND}}(g_m, \phi), \mathbf{u}_{\text{ND}}(0, \delta\phi) \rangle, \end{aligned}$$

and use the properties of the maps \mathbf{u}_{DN} and \mathbf{u}_{ND} given in Proposition 3.1 to express each of the previous expressions as integrals over the inner boundary. We first consider products of the same map. On the one hand, we have

$$\begin{aligned} \langle \mathbf{u}_{\text{DN}}(f_m, \psi), \mathbf{u}_{\text{DN}}(0, \delta\psi) \rangle &= \int_{\partial\Omega} f_m \partial_{\mathbf{n}} \mathbf{u}_{\text{DN}}(0, \delta\psi) + \int_{\partial\omega} \mathbf{u}_{\text{DN}}(f_m, \psi) \delta\psi \\ &= - \int_{\partial\omega} \mathbf{u}_{\text{DN}}(f_m, 0) \delta\psi + \int_{\partial\omega} \mathbf{u}_{\text{DN}}(f_m, \psi) \delta\psi \\ &= \int_{\partial\omega} [\mathbf{u}_{\text{DN}}(f_m, \psi) - \mathbf{u}_{\text{DN}}(f_m, 0)] \delta\psi \\ &= \int_{\partial\omega} \mathbf{u}_{\text{DN}}(0, \psi) \delta\psi. \end{aligned}$$

On the other hand, we get in a similar manner

$$\begin{aligned} \langle \mathbf{u}_{\text{ND}}(g_m, \phi), \mathbf{u}_{\text{ND}}(0, \delta\phi) \rangle &= \int_{\partial\Omega} \mathbf{u}_{\text{ND}}(0, \delta\phi) g_m + \int_{\partial\omega} \delta\phi \partial_{\mathbf{n}} \mathbf{u}_{\text{ND}}(g_m, \phi) \\ &= - \int_{\partial\Omega} \delta\phi \partial_{\mathbf{n}} \mathbf{u}_{\text{ND}}(g_m, 0) + \int_{\partial\omega} \delta\phi \partial_{\mathbf{n}} \mathbf{u}_{\text{ND}}(g_m, \phi) \\ &= \int_{\partial\Omega} \delta\phi \partial_{\mathbf{n}} [\mathbf{u}_{\text{ND}}(g_m, \phi) - \mathbf{u}_{\text{ND}}(g_m, 0)] \\ &= \int_{\partial\Omega} \delta\phi \partial_{\mathbf{n}} \mathbf{u}_{\text{ND}}(0, \phi). \end{aligned}$$

Then, we consider the mixed products

$$\begin{aligned} \langle \mathbf{u}_{\text{DN}}(f_m, \psi), \mathbf{u}_{\text{ND}}(0, \delta\phi) \rangle &= \int_{\partial\Omega} \mathbf{u}_{\text{ND}}(0, \delta\phi) \partial_{\mathbf{n}} \mathbf{u}_{\text{DN}}(f_m, \psi) + \int_{\partial\omega} \psi \delta\phi \\ &= - \int_{\partial\omega} \partial_{\mathbf{n}} \mathbf{u}_{\text{ND}}(\partial_{\mathbf{n}} \mathbf{u}_{\text{DN}}(f_m, \psi), 0) \delta\phi + \int_{\partial\omega} \psi \delta\phi \\ &= \int_{\partial\omega} [\psi - \partial_{\mathbf{n}} \mathbf{u}_{\text{ND}}(\partial_{\mathbf{n}} \mathbf{u}_{\text{DN}}(f_m, \psi), 0)] \delta\phi, \end{aligned}$$

and in the very same manner

$$\begin{aligned} \langle \mathbf{u}_{\text{ND}}(g_m, \phi), \mathbf{u}_{\text{DN}}(0, \delta\psi) \rangle &= \int_{\partial\Omega} \mathbf{u}_{\text{ND}}(g_m, \phi) \partial_{\mathbf{n}} \mathbf{u}_{\text{DN}}(0, \delta\psi) \int_{\partial\omega} \phi \delta\psi \\ &= \int_{\partial\omega} [\phi - \mathbf{u}_{\text{DN}}(\mathbf{u}_{\text{ND}}(g_m, \phi), 0)] \delta\psi. \end{aligned}$$

Gathering the terms, we obtain the announced expression of the gradient.

□

REMARK 3.4. *As seen from the previous proof, we have*

$$\begin{aligned} D^2\mathcal{K}(\phi, \psi) \cdot ([\delta\phi_1, \delta\psi_1], [\delta\phi_2, \delta\psi_2]) &= D\mathcal{K}(\delta\phi_1, \delta\psi_1) \cdot ([\delta\phi_2, \delta\psi_2]) \\ &= D\mathcal{K}(\delta\phi_2, \delta\psi_2) \cdot ([\delta\phi_1, \delta\psi_1]). \end{aligned}$$

Thus, the Hessian does not depend on (ϕ, ψ) . Especially, it holds

$$\begin{aligned} D^2\mathcal{K}(\phi, \psi) \cdot ([\delta\phi_1, \delta\psi_1], [\delta\phi_2, \delta\psi_2]) &= \int_{\partial\omega} [\partial_{\mathbf{n}}\mathbf{u}_{\text{ND}}(\partial_{\mathbf{n}}\mathbf{u}_{\text{DN}}(0, \delta\psi_1), \delta\phi_1) - \delta\psi_1] \delta\phi_1 \\ &\quad + [\mathbf{u}_{\text{DN}}(\mathbf{u}_{\text{ND}}(0, \delta\phi_2), \delta\psi_2) - \delta\phi_2] \delta\psi_2. \end{aligned}$$

4. Numerical resolution of the data completion problem.

4.1. Newton scheme. As mentioned previously, a regularization process is needed for such a severely ill-posed inverse problem. We use here the standard Tikhonov regularization as studied, e.g., in [16]. Therefore, we consider a non-negative real number ε and introduce the regularized Kohn-Vogelius cost functional $\mathcal{K}^\varepsilon : H^{1/2}(\partial\omega) \times H^{-1/2}(\partial\omega) \rightarrow \mathbb{R}$ defined by

$$(4.1) \quad \mathcal{K}^\varepsilon(\phi, \psi) = \mathcal{K}(\phi, \psi) + \varepsilon\mathcal{T}(\phi, \psi),$$

where the regularizing term $\mathcal{T}(\phi, \psi)$ is defined by

$$\begin{aligned} \mathcal{T}(\phi, \psi) &:= \frac{1}{2} \left(|\mathbf{u}_{\text{ND}}(0, \phi)|_{H^1(\Omega \setminus \bar{\omega})}^2 + |\mathbf{u}_{\text{DN}}(0, \psi)|_{H^1(\Omega \setminus \bar{\omega})}^2 + \int_{\partial\omega} \phi^2 \right) \\ &= \frac{1}{2} \int_{\partial\omega} (\phi + \partial_{\mathbf{n}}\mathbf{u}_{\text{ND}}(0, \phi))\phi + \mathbf{u}_{\text{DN}}(0, \psi)\psi. \end{aligned}$$

LEMMA 4.1. *The regularizing functional \mathcal{T} is non-negative with the unique minimizer $(0, 0)$.*

Proof. Assume that (ϕ, ψ) is such that

$$|\mathbf{u}_{\text{ND}}(0, \phi)|_{H^1(\Omega \setminus \bar{\omega})}^2 + |\mathbf{u}_{\text{DN}}(0, \psi)|_{H^1(\Omega \setminus \bar{\omega})}^2 = 0.$$

Then, $\mathbf{u}_{\text{ND}}(0, \phi)$ and $\mathbf{u}_{\text{DN}}(0, \psi)$ are constant functions. By exploiting the boundary conditions on $\partial\omega$, we check that ϕ is constant and $\psi = 0$ on $\partial\omega$. Hence $\phi = \psi = 0$ is a minimizer and the proof is complete. □

REMARK 4.2. *This regularization permits to obtain the existence of a unique minimizer, for all $\varepsilon > 0$, even for not compatible data thanks to the gained of coerciveness and, in case of compatible data, the convergence of these minimizers towards the exact solution when ε goes to 0 (see, e.g., [16, Proposition 2.5 and Theorem 2.6]).*

REMARK 4.3. *Notice that the usual regularizing term would have been the term $\|(\phi, \psi)\|_{H^{1/2}(\partial\omega) \times H^{-1/2}(\partial\omega)}^2$, but the two quantities are equivalent as claimed in the following lemma.*

LEMMA 4.4. *There exist two non-negative constants C_1 and C_2 such that*

$$C_1 \|\psi\|_{H^{-1/2}(\partial\omega)}^2 \leq |\mathbf{u}_{\text{DN}}(0, \psi)|_{H^1(\Omega \setminus \bar{\omega})}^2 \leq C_2 \|\psi\|_{H^{-1/2}(\partial\omega)}^2$$

and

$$C_1 \|\phi\|_{\mathbf{H}^{1/2}(\partial\omega)}^2 \leq |\mathbf{u}_{\text{ND}}(0, \phi)|_{\mathbf{H}^1(\Omega \setminus \bar{\omega})}^2 + \int_{\partial\omega} \phi^2 \leq C_2 \|\phi\|_{\mathbf{H}^{1/2}(\partial\omega)}^2,$$

for all $(\phi, \psi) \in \mathbf{H}^{1/2}(\partial\omega) \times \mathbf{H}^{-1/2}(\partial\omega)$.

Proof. Firstly, thanks to the continuity of the trace operator and thanks to Proposition 3.1 (see equation (3.1)), there exists two non-negative constants C_1 and C_2 such that

$$C_1 \|\psi\|_{\mathbf{H}^{-1/2}(\partial\omega)}^2 \leq \|\mathbf{u}_{\text{DN}}(0, \psi)\|^2 \leq C_2 \|\psi\|_{\mathbf{H}^{-1/2}(\partial\omega)}^2,$$

for all $\psi \in \mathbf{H}^{-1/2}(\partial\omega)$. Since $\mathbf{u}_{\text{DN}}(0, \psi) = 0$ on $\partial\Omega$, Poincaré's inequality ensures that the semi-norm is equivalent to the \mathbf{H}^1 -norm. Hence, we obtain the following inequalities (for others constants still denoted by C_1 and C_2)

$$C_1 \|\psi\|_{\mathbf{H}^{-1/2}(\partial\omega)}^2 \leq |\mathbf{u}_{\text{DN}}(0, \psi)|_{\mathbf{H}^1(\Omega \setminus \bar{\omega})}^2 \leq C_2 \|\psi\|_{\mathbf{H}^{-1/2}(\partial\omega)}^2.$$

Secondly, using again (3.1) and the continuous embedding $\mathbf{H}^{1/2}(\partial\omega) \hookrightarrow \mathbf{L}^2(\partial\omega)$, there exists a non-negative constant C_3 such that

$$|\mathbf{u}_{\text{ND}}(0, \phi)|_{\mathbf{H}^1(\Omega \setminus \bar{\omega})}^2 + \int_{\partial\omega} \phi^2 \leq C_3 \|\phi\|_{\mathbf{H}^{1/2}(\partial\omega)}^2,$$

for all $\phi \in \mathbf{H}^{1/2}(\partial\omega)$.

Let us now show that there exists a non-negative constant C_4 such that

$$C_4 \|\mathbf{u}_{\text{ND}}(0, \phi)\|_{\mathbf{H}^1(\Omega \setminus \bar{\omega})}^2 \leq |\mathbf{u}_{\text{ND}}(0, \phi)|_{\mathbf{H}^1(\Omega \setminus \bar{\omega})}^2 + \int_{\partial\omega} \phi^2,$$

for all $\phi \in \mathbf{H}^{1/2}(\partial\omega)$, which will complete the proof by using the continuity of the trace operator. To this end, let us proceed by contradiction assuming that, for all $n \in \mathbb{N}$, there exists $\phi_n \in \mathbf{H}^{1/2}(\partial\omega)$ such that

$$\|v_n\|_{\mathbf{H}^1(\Omega \setminus \bar{\omega})} = 1 \quad \text{and} \quad \frac{1}{n} > |v_n|_{\mathbf{H}^1(\Omega \setminus \bar{\omega})}^2 + \int_{\partial\omega} v_n^2,$$

where we have set $v_n := \frac{\mathbf{u}_{\text{ND}}(0, \phi)}{\|\mathbf{u}_{\text{ND}}(0, \phi)\|_{\mathbf{H}^1(\Omega \setminus \bar{\omega})}}$. Hence, $\|\nabla v_n\|_{\mathbf{H}^1(\Omega \setminus \bar{\omega})} \xrightarrow{n \rightarrow +\infty} 0$ and

$\int_{\partial\omega} v_n^2 \xrightarrow{n \rightarrow +\infty} 0$. Furthermore, $(v_n)_n$ is bounded in $\mathbf{H}^1(\Omega \setminus \bar{\omega})$ which is compactly embedded in $\mathbf{L}^2(\Omega \setminus \bar{\omega})$ and then, up to a subsequence, there exists $v \in \mathbf{H}^1(\Omega \setminus \bar{\omega})$ such that

$$v_n \rightharpoonup v \text{ in } \mathbf{H}^1(\Omega \setminus \bar{\omega}) \quad \text{and} \quad v_n \rightarrow v \text{ in } \mathbf{L}^2(\Omega \setminus \bar{\omega}).$$

Since $\nabla v_n \rightarrow \mathbf{0}$ in $\mathbf{L}^2(\Omega \setminus \bar{\omega})$, we conclude that $v_n \rightarrow v$ in $\mathbf{H}^1(\Omega \setminus \bar{\omega})$ and $\nabla v = \mathbf{0}$. Therefore, v is constant and

$$\int_{\partial\omega} v_n^2 \rightarrow 0 = \int_{\partial\omega} v^2 = v^2 |\partial\omega|.$$

Thus, $v = 0$ which contradicts the fact that $\|v_n\| = 1 \rightarrow \|v\| = 1$. \square

We now compute the gradient of the objectives with respect to (ϕ, ψ) .

PROPOSITION 4.5. *The derivatives of \mathcal{T} with respect to (ϕ, ψ) are*

$$D\mathcal{T}(\phi, \psi) \cdot [\delta\phi, \delta\psi] = \int_{\partial\omega} \delta\phi(\phi + \partial_{\mathbf{n}}\mathbf{u}_{\text{ND}}(0, \phi)) + \mathbf{u}_{\text{DN}}(0, \psi)\delta\psi$$

and

$$\begin{aligned} D^2\mathcal{T}(\phi, \psi) \cdot [(\delta\phi_1, \delta\psi_1), (\delta\phi_2, \delta\psi_2)] \\ = \int_{\partial\omega} \delta\phi_1(\delta\phi_2 + \partial_{\mathbf{n}}\mathbf{u}_{\text{ND}}(0, \delta\phi_2)) + \mathbf{u}_{\text{ND}}(0, \delta\psi_2)\delta\psi_1. \end{aligned}$$

Proof. We expand the quadratic quantity \mathcal{T} and follow the proof of Proposition 3.3 to get the announced result. \square

REMARK 4.6. *The first idea to build a numerical scheme for minimizing the objective is to use a descent method. This leads to a sequence (ϕ_n, ψ_n) by the update rule*

$$\begin{pmatrix} \phi_{n+1} \\ \psi_{n+1} \end{pmatrix} = \begin{pmatrix} \phi_n \\ \psi_n \end{pmatrix} + \tau_{n+1}\mathbf{d}_n,$$

where τ_{n+1} is a descent step and where the descent direction \mathbf{d}_n is naturally chosen as the formal anti-gradient:

$$\mathbf{d}_n = - \begin{pmatrix} \partial_{\mathbf{n}}\mathbf{u}_{\text{ND}}(\partial_{\mathbf{n}}\mathbf{u}_{\text{DN}}(f_m, \psi_n), \phi_n) - \psi_n \\ \mathbf{u}_{\text{DN}}(\mathbf{u}_{\text{ND}}(g_m, \psi_n), \psi_n) - \phi_n \end{pmatrix} + \varepsilon \begin{pmatrix} \phi_n + \partial_{\mathbf{n}}\mathbf{u}_{\text{ND}}(0, \phi_n) \\ \mathbf{u}_{\text{DN}}(0, \psi_n) \end{pmatrix}.$$

In fact, \mathbf{d}_n is not the gradient of \mathcal{K} . Indeed, the true gradient should be computed with respect to the scalar product on $\mathbf{H}^{1/2}(\partial\omega) \times \mathbf{H}^{-1/2}(\partial\omega)$ and not with respect to $\mathbf{L}^2(\partial\omega) \times \mathbf{L}^2(\partial\omega)$. A nice way to see that is that this updates is not in the right spaces: while $(\phi_n, \psi_n) \in \mathbf{H}^{1/2}(\partial\omega) \times \mathbf{H}^{-1/2}(\partial\omega)$, the update \mathbf{d}_n lies in $\mathbf{H}^{-1/2}(\partial\omega) \times \mathbf{H}^{1/2}(\partial\omega)$.

The true gradient is much more complex to compute at least at the continuous level. Therefore, we will not consider the gradient method here and directly solve the linearized equation. This is the idea of Newton method.

PROPOSITION 4.7. *The Newton update $(\delta\phi, \delta\psi) \in \mathbf{H}^{1/2}(\partial\omega) \times \mathbf{H}^{-1/2}(\partial\omega)$ for the regularized Kohn-Vogelius objective $\mathcal{K}^\varepsilon(\phi_n, \psi_n)$ is given by the linear system*

$$\begin{cases} \partial_{\mathbf{n}}\mathbf{u}_{\text{ND}}(\partial_{\mathbf{n}}\mathbf{u}_{\text{DN}}(0, \delta\psi), \delta\phi) - \delta\psi + \varepsilon(\delta\phi + \partial_{\mathbf{n}}\mathbf{u}_{\text{ND}}(0, \delta\phi)) \\ \quad = \psi_n - \partial_{\mathbf{n}}\mathbf{u}_{\text{ND}}(\partial_{\mathbf{n}}\mathbf{u}_{\text{DN}}(f_m, \psi_n), \phi_n) - \varepsilon(\phi_n + \partial_{\mathbf{n}}\mathbf{u}_{\text{ND}}(0, \phi_n)), \\ \mathbf{u}_{\text{DN}}(\mathbf{u}_{\text{ND}}(0, \delta\phi), \delta\psi) - \delta\phi + \varepsilon\mathbf{u}_{\text{DN}}(0, \delta\psi) \\ \quad = \phi_n - \mathbf{u}_{\text{DN}}(\mathbf{u}_{\text{ND}}(g_m, \psi_n), \psi_n) - \varepsilon\mathbf{u}_{\text{DN}}(0, \psi_n). \end{cases}$$

Proof. The Newton scheme leads to the sequence (ϕ_n, ψ_n) such that the increment

$$(\delta\phi, \delta\psi) = (\phi_{n+1}, \psi_{n+1}) - (\phi_n, \psi_n)$$

satisfies the weak problem

$$(D^2\mathcal{K} + \varepsilon D^2\mathcal{T})(\phi_n, \psi_n) \cdot [(\delta\phi, \delta\psi), [h, \ell]] = -(D\mathcal{K} + \varepsilon D\mathcal{T})(\phi_n, \psi_n) \cdot [h, \ell]$$

for all $[h, \ell] \in \mathbf{H}^{1/2}(\partial\omega) \times \mathbf{H}^{-1/2}(\partial\omega)$.

To solve this equation in the unknowns $(\delta\phi, \delta\psi)$, we need to rewrite the left hand side in order to make explicit the dependency on $[h, \ell]$. We proceed as for the gradient: we first expand

$$\begin{aligned} & \langle \mathbf{u}_{\text{DN}}(0, \delta\psi) - \mathbf{u}_{\text{ND}}(0, \delta\phi), \mathbf{u}_{\text{DN}}(0, \ell) - \mathbf{u}_{\text{ND}}(0, h) \rangle \\ &= \langle \mathbf{u}_{\text{DN}}(0, \delta\psi), \mathbf{u}_{\text{DN}}(0, \ell) \rangle + \langle \mathbf{u}_{\text{ND}}(0, \delta\phi), \mathbf{u}_{\text{ND}}(0, h) \rangle \\ & \quad - \langle \mathbf{u}_{\text{ND}}(0, \delta\phi), \mathbf{u}_{\text{DN}}(0, \ell) \rangle - \langle \mathbf{u}_{\text{DN}}(0, \delta\psi), \mathbf{u}_{\text{ND}}(0, h) \rangle \end{aligned}$$

and then compute each term:

$$\begin{aligned} \langle \mathbf{u}_{\text{DN}}(0, \delta\psi), \mathbf{u}_{\text{DN}}(0, \ell) \rangle &= \int_{\partial\omega} \mathbf{u}_{\text{DN}}(0, \delta\psi) \ell, \\ \langle \mathbf{u}_{\text{ND}}(0, \delta\phi), \mathbf{u}_{\text{ND}}(0, h) \rangle &= \int_{\partial\omega} \partial_{\mathbf{n}} \mathbf{u}_{\text{ND}}(0, \delta\phi) h, \\ \langle \mathbf{u}_{\text{ND}}(0, \delta\phi), \mathbf{u}_{\text{DN}}(0, \ell) \rangle &= \int_{\partial\omega} [\delta\phi - \mathbf{u}_{\text{DN}}(\mathbf{u}_{\text{ND}}(0, \delta\phi), 0)] \ell, \\ \langle \mathbf{u}_{\text{DN}}(0, \delta\psi), \mathbf{u}_{\text{ND}}(0, h) \rangle &= \int_{\partial\omega} [\delta\psi - \partial_{\mathbf{n}} \mathbf{u}_{\text{ND}}(\partial_{\mathbf{n}} \mathbf{u}_{\text{DN}}(0, \delta\psi), 0)] h. \end{aligned}$$

The weak problem reads: find $(\delta\phi, \delta\psi) \in \mathbf{H}^{1/2}(\partial\omega) \times \mathbf{H}^{-1/2}(\partial\omega)$ such that

$$\begin{aligned} & \int_{\partial\omega} [\mathbf{u}_{\text{DN}}(\mathbf{u}_{\text{ND}}(0, \delta\phi), \delta\psi) - \delta\phi + \varepsilon \mathbf{u}_{\text{DN}}(0, \delta\psi)] \ell \\ & \quad + [\partial_{\mathbf{n}} \mathbf{u}_{\text{ND}}(\partial_{\mathbf{n}} \mathbf{u}_{\text{DN}}(0, \delta\psi), \delta\phi) - \delta\psi + \varepsilon (\delta\phi + \partial_{\mathbf{n}} \mathbf{u}_{\text{ND}}(0, \delta\phi))] h \\ &= - \int_{\partial\omega} [\partial_{\mathbf{n}} \mathbf{u}_{\text{ND}}(\partial_{\mathbf{n}} \mathbf{u}_{\text{DN}}(f_{\text{m}}, \psi_n), \phi_n) - \psi_n + \varepsilon (\phi_n + \partial_{\mathbf{n}} \mathbf{u}_{\text{ND}}(0, \phi_n))] h \\ & \quad - \int_{\partial\omega} [\mathbf{u}_{\text{DN}}(\mathbf{u}_{\text{ND}}(g_{\text{m}}, \psi_n), \psi_n) - \phi_n + \varepsilon \mathbf{u}_{\text{DN}}(0, \psi_n)] \ell \end{aligned}$$

for all $(h, \ell) \in \mathbf{H}^{1/2}(\partial\omega) \times \mathbf{H}^{-1/2}(\partial\omega)$. This implies the assertion. \square

4.2. Implementation. Our approach to determine the Cauchy data of the functions $\mathbf{u}_{\text{DN}}(f_{\text{m}}, \psi)$ and $\mathbf{u}_{\text{ND}}(g_{\text{m}}, \phi)$ relies on a system of boundary integral equations arising from the direct formulation based on Green's fundamental solution.

In this section, in order to simplify the formulae, we use the following notation: $\Sigma := \partial\Omega$ and $\Gamma := \partial\omega$.

Assuming that $u \in \mathbf{H}^1(\Omega \setminus \bar{\omega})$ solves Laplace's equation, then Green's representation formula implies the relation

$$u(\mathbf{x}) = \int_{\Sigma \cup \Gamma} \left\{ G(\mathbf{x}, \mathbf{y}) \frac{\partial u}{\partial \mathbf{n}}(\mathbf{y}) - \frac{\partial G(\mathbf{x}, \mathbf{y})}{\partial \mathbf{n}_{\mathbf{y}}} u(\mathbf{y}) \right\} d\sigma_{\mathbf{y}}, \quad \mathbf{x} \in \Omega \setminus \bar{\omega},$$

where the Green function G is given by

$$G(\mathbf{x}, \mathbf{y}) = \begin{cases} -\frac{1}{2\pi} \log |\mathbf{x} - \mathbf{y}|, & \text{if } d = 2, \\ \frac{1}{4\pi |\mathbf{x} - \mathbf{y}|}, & \text{if } d = 3. \end{cases}$$

Using the jump properties of the layer potentials, we obtain the direct boundary integral formulation of the problem

$$(4.2) \quad u(\mathbf{x}) = \int_{\Gamma \cup \Sigma} G(\mathbf{x}, \mathbf{y}) \frac{\partial u}{\partial \mathbf{n}}(\mathbf{y}) d\sigma_{\mathbf{y}} + \frac{1}{2} u(\mathbf{x}) - \int_{\Gamma \cup \Sigma} \frac{\partial G(\mathbf{x}, \mathbf{y})}{\partial \mathbf{n}_{\mathbf{y}}} u(\mathbf{y}) d\sigma_{\mathbf{y}}, \quad \mathbf{x} \in \Gamma \cup \Sigma.$$

We restrict ourselves to the two-dimensional situation $d = 2$.

Let $A, B \in \{\Gamma, \Sigma\}$ which represent the boundaries. Then the expression (4.2) includes the single layer operator defined by

$$(4.3) \quad S : \mathcal{C}(A) \rightarrow \mathcal{C}(B), \quad (S_{AB})(\rho)(\mathbf{x}) = -\frac{1}{2\pi} \int_A \log |\mathbf{x} - \mathbf{y}| \rho(\mathbf{y}) d\sigma_{\mathbf{y}},$$

and the double layer operator defined by

$$(4.4) \quad D : \mathcal{C}(A) \rightarrow \mathcal{C}(B), \quad (D_{AB})(\rho)(\mathbf{x}) = \frac{1}{2\pi} \int_A \frac{\langle \mathbf{x} - \mathbf{y}, \mathbf{n}_{\mathbf{y}} \rangle}{|\mathbf{x} - \mathbf{y}|^2} \rho(\mathbf{y}) d\sigma_{\mathbf{y}},$$

with the densities ρ being the Cauchy data of u at the boundary A . The equation (4.2) in combination with (4.3) and (4.4) amounts to the Dirichlet-to-Neumann map, which is given by the following system of integral equations

$$\begin{bmatrix} S_{\Gamma\Gamma} & S_{\Sigma\Gamma} \\ S_{\Gamma\Sigma} & S_{\Sigma\Sigma} \end{bmatrix} \begin{bmatrix} \partial_{\mathbf{n}} u|_{\Gamma} \\ \partial_{\mathbf{n}} u|_{\Sigma} \end{bmatrix} = \begin{bmatrix} \frac{1}{2}\mathbf{I} + D_{\Gamma\Gamma} & D_{\Sigma\Gamma} \\ D_{\Gamma\Sigma} & \frac{1}{2}\mathbf{I} + D_{\Sigma\Sigma} \end{bmatrix} \begin{bmatrix} u|_{\Gamma} \\ u|_{\Sigma} \end{bmatrix}.$$

Reordering this system of boundary integral equations yields the missing Cauchy data of the solution $\mathbf{u}_{\text{DN}}(f_m, \psi) \in \mathbf{H}^1(\Omega \setminus \bar{\omega})$ of problem (2.3) by

$$(4.5) \quad \begin{bmatrix} \frac{1}{2}\mathbf{I} + D_{\Gamma\Gamma} & -S_{\Sigma\Gamma} \\ -D_{\Gamma\Sigma} & S_{\Sigma\Sigma} \end{bmatrix} \begin{bmatrix} u|_{\Gamma} \\ \partial_{\mathbf{n}} u|_{\Sigma} \end{bmatrix} = \begin{bmatrix} S_{\Gamma\Gamma} & -D_{\Sigma\Gamma} \\ -S_{\Gamma\Sigma} & \frac{1}{2}\mathbf{I} + D_{\Sigma\Sigma} \end{bmatrix} \begin{bmatrix} \psi \\ f_m \end{bmatrix}$$

and of the solution $\mathbf{u}_{\text{ND}}(g_m, \phi) \in \mathbf{H}^1(\Omega \setminus \bar{\omega})$ of Problem (2.4) by

$$(4.6) \quad \begin{bmatrix} S_{\Gamma\Gamma} & -D_{\Sigma\Gamma} \\ -S_{\Gamma\Sigma} & \frac{1}{2}\mathbf{I} + D_{\Sigma\Sigma} \end{bmatrix} \begin{bmatrix} \partial_{\mathbf{n}} u|_{\Gamma} \\ u|_{\Sigma} \end{bmatrix} = \begin{bmatrix} \frac{1}{2}\mathbf{I} + D_{\Gamma\Gamma} & -S_{\Sigma\Gamma} \\ -D_{\Gamma\Sigma} & S_{\Sigma\Sigma} \end{bmatrix} \begin{bmatrix} \phi \\ g_m \end{bmatrix}.$$

The boundary integral operators on the left hand side of the systems (4.5) and (4.6) of boundary integral equations are continuous and satisfy a Gårding inequality with respect to $L^2(\Gamma) \times \mathbf{H}^{-1/2}(\Sigma)$ and $\mathbf{H}^{-1/2}(\Gamma) \times L^2(\Sigma)$, respectively, provided that $\text{diam}(\Omega) < 1$. Since injectivity follows from potential theory, these systems of integral equations are uniquely solvable according to the Riesz-Schauder theory. With the help of the solutions given by (4.5) and (4.6), we can compute the Kohn-Vogelius functional (3.2) and its gradient and Hessian. The same holds true for the regularized functional \mathcal{K}^ε .

The next step towards the solution of the boundary value problem is the numerical approximation of the integral operators included in (4.5) and (4.6), respectively, which first requires the parametrization of the integral equations. To that end, we insert parameterizations $\gamma : [0, 2\pi] \rightarrow \Gamma$ and $\sigma : [0, 2\pi] \rightarrow \Sigma$ of the boundaries. For the approximation of the unknown Cauchy data, we use the collocation method based on trigonometric polynomials. Applying the trapezoidal rule for the numerical quadrature and the regularization technique along the lines of [34] to deal with the singular

integrals, we arrive at an exponentially convergent boundary element method provided that the data and the boundaries and thus the solution are arbitrarily smooth.

Since the Hessian of the functional $\mathcal{K}^\varepsilon(\phi, \psi)$ does not depend on the argument (ϕ, ψ) , the Newton scheme converges in one iteration. Especially, the Hessian is positive definite since the functional under consideration is convex. We can thus use the conjugate gradient method [30] to compute the Newton update. Therefore, we can efficiently determine the functions $(\phi, \psi) \in \mathbf{H}^{1/2}(\Gamma) \times \mathbf{H}^{-1/2}(\Gamma)$ such that it holds $\mathbf{u}_{\text{ND}}(g_m, \phi) = \mathbf{u}_{\text{DN}}(f_m, \psi)$ for the current boundary $\Gamma = \partial\omega$.

4.3. Numerical validation. We shall validate the data completion approach by some numerical test examples. We choose Ω as the ball of radius 0.4, which is centered in $\mathbf{0}$. If we take the Cauchy data of a known harmonic function u at the outer boundary $\partial\Omega$ as data (f_m, g_m) , the desired Cauchy data $(\phi, \psi) \in \mathbf{H}^{1/2}(\partial\omega) \times \mathbf{H}^{-1/2}(\partial\omega)$ at the inclusion's boundary $\partial\omega$ are just $(u|_{\partial\omega}, \partial_{\mathbf{n}}u|_{\partial\omega})$.

The settings for the data completion algorithm are as follows. The regularization parameter ε for the data completion functional (4.1) is set to $\varepsilon = 0.1$, $\varepsilon = 0.01$, or $\varepsilon = 0.001$. We use $N = 200$ boundary elements per boundary for the discretization of the boundary integral equations in (4.5) and (4.6), respectively. Hence, the computed Cauchy data (ϕ_N, ψ_N) at the inclusion's boundary $\partial\omega$ are represented by $N = 200$ boundary elements each.

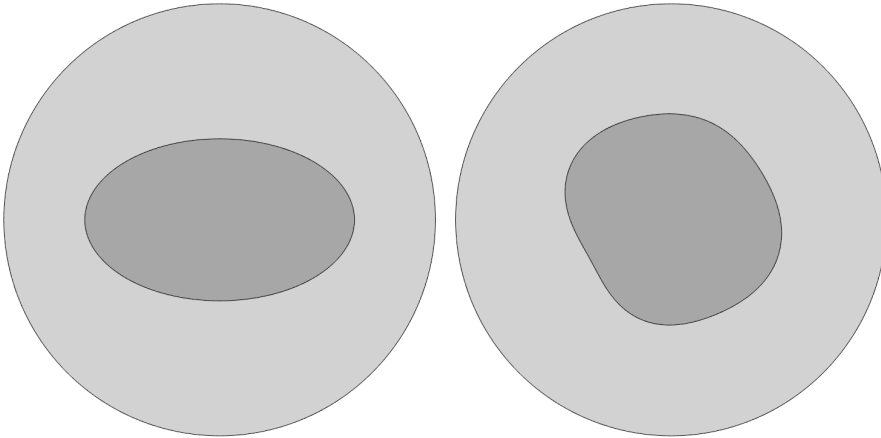


FIG. 4.1. The ball with ellipse inclusion (left-hand side) and with potato inclusion (right-hand side).

In our first example, we consider the ellipse with semi-axis $h_x = 0.25$ and $h_y = 0.15$ as inclusion ω , compare the left plot of Figure 4.1. In the second example, we have a potato shaped inclusion ω , compare the right plot of Figure 4.1. We moreover prescribe the Cauchy data (f_m, g_m) of the harmonic function $u(x, y) = x^2 - y^2$. The approximation errors for the different geometries and regularization parameters are found in Table 4.1, where the respective Sobolev norms are computed by means of appropriately weighted Fourier series. In particular, we observe that the best choice for the regularization parameter is $\varepsilon = 0.01$ since therefore the approximation errors are the smallest ones. We like to stress that an increase of the number N of boundary elements does not increase accuracy, which reflects the severe ill-posedness of the problem under consideration. We like to mention that, adding noise to the Neumann

data g_m as described in the next section, does not significantly change the results found in Table 4.1.

		regularization parameter	$\varepsilon = 0.1$	$\varepsilon = 0.05$	$\varepsilon = 0.01$	$\varepsilon = 0.005$	$\varepsilon = 0.001$
ellipse	$\frac{\ \phi - \phi_N\ _{\mathbf{H}^{1/2}(\Gamma)}}{\ \phi\ _{\mathbf{H}^{1/2}(\Gamma)}}$		$1.7256 \cdot 10^{-1}$	$1.5610 \cdot 10^{-1}$	$1.4621 \cdot 10^{-1}$	$2.3244 \cdot 10^{-1}$	$2.3302 \cdot 10^{-1}$
	$\frac{\ \psi - \psi_N\ _{\mathbf{H}^{-1/2}(\Gamma)}}{\ \psi\ _{\mathbf{H}^{-1/2}(\Gamma)}}$		$1.3689 \cdot 10^{-2}$	$1.3586 \cdot 10^{-2}$	$7.7903 \cdot 10^{-3}$	$1.2139 \cdot 10^{-1}$	$1.2085 \cdot 10^{-1}$
potato	$\frac{\ \phi - \phi_N\ _{\mathbf{H}^{1/2}(\Gamma)}}{\ \phi\ _{\mathbf{H}^{1/2}(\Gamma)}}$		$8.0964 \cdot 10^{-2}$	$5.0993 \cdot 10^{-2}$	$8.1978 \cdot 10^{-2}$	$8.4939 \cdot 10^{-2}$	$8.7713 \cdot 10^{-2}$
	$\frac{\ \psi - \psi_N\ _{\mathbf{H}^{-1/2}(\Gamma)}}{\ \psi\ _{\mathbf{H}^{-1/2}(\Gamma)}}$		$4.2829 \cdot 10^{-2}$	$2.6365 \cdot 10^{-2}$	$3.5529 \cdot 10^{-2}$	$3.6279 \cdot 10^{-2}$	$3.7131 \cdot 10^{-2}$

TABLE 4.1

The approximation errors for the data completion approach in dependence of the regularization parameter.

5. Resolution of the inverse obstacle problem with the trial method.

We now aim to numerically solve the inverse obstacle problem (1.1). The general idea is to use the previous data completion step in order to reconstruct $u|_{\partial\omega}$ and $\partial_{\mathbf{n}}u|_{\partial\omega}$ on an approximation $\partial\omega$ of the *real* inclusion and then to use the so-called *trial method* in order to update the shape of the inclusion.

We first present the *trial method* and then illustrate the efficiency of our method with some numerical simulations.

5.1. Background and motivation. The trial method is a fixed-point type iterative method, which is well-known from the solution of free boundary problems (see, e.g., [9, 22, 42] and the references therein). In the context of inverse problems, it has been used for example in [41].

We shall assume in the following that the domain ω is starlike. Hence, we can represent the inclusion's boundary $\partial\omega$ by a parametrization $\gamma : [0, 2\pi] \rightarrow \mathbb{R}^2$ in polar coordinates, that is

$$\partial\omega = \{\gamma(s) = r(s)\mathbf{e}_r(s); s \in [0, 2\pi]\},$$

where $\mathbf{e}_r(s) = (\cos(s), \sin(s))^\top$ denotes the unit vector in the radial direction. The radial function $r(s)$ is supposed to be a positive function in $\mathcal{C}_{\text{per}}([0, 2\pi])$, where

$$\mathcal{C}_{\text{per}}([0, 2\pi]) = \{r \in \mathcal{C}([0, 2\pi]); r(0) = r(2\pi)\},$$

such that $\text{dist}(\partial\Omega, \partial\omega) > 0$.

The trial method to solve the conductivity problem (1.1) requires an update rule. Suppose that the actual void's boundary is $\partial\omega_k$. Then the data completion problem yields a state u_k which satisfies

$$\begin{cases} \Delta u_k = 0 & \text{in } \Omega \setminus \overline{\omega_k}, \\ u_k = f_m & \text{on } \partial\Omega, \\ \partial_{\mathbf{n}} u_k = g_m & \text{on } \partial\Omega. \end{cases}$$

The new boundary $\partial\omega_{k+1}$ is now determined by moving the old boundary into the radial direction, which is expressed by the update rule

$$(5.1) \quad \gamma_{k+1} = \gamma_k + \delta r_k \mathbf{e}_r.$$

The computation of the update function δr_k is the topic of the next section.

5.2. Update rule. The update function $\delta r_k \in \mathcal{C}_{\text{per}}([0, 2\pi])$ should be constructed in such a way that the desired homogeneous Dirichlet boundary condition will be (approximately) satisfied at the new boundary $\partial\omega_{k+1}$, i.e.,

$$u_k \circ \gamma_{k+1} \stackrel{!}{=} 0 \quad \text{on } [0, 2\pi],$$

where u_k is assumed to be smoothly extended into the exterior of $\Omega \setminus \bar{\omega}_k$ if required.

The traditional update rule is obtained by linearizing $u_k \circ (\gamma_k + \delta r_k \mathbf{e}_r)$ with respect to the update function δr . This yields the equation

$$u_k \circ \gamma_{k+1} \approx u_k \circ \gamma_k + \left(\frac{\partial u_k}{\partial \mathbf{e}_r} \circ \gamma_k \right) \delta r_k.$$

We decompose the derivative of u_k in the direction \mathbf{e}_r into its normal and tangential components:

$$\frac{\partial u_k}{\partial \mathbf{e}_r} = \frac{\partial u_k}{\partial \mathbf{n}} \langle \mathbf{e}_r, \mathbf{n} \rangle + \frac{\partial u_k}{\partial \mathbf{t}} \langle \mathbf{e}_r, \mathbf{t} \rangle \quad \text{on } \partial\omega_k.$$

Hence, defining $F(\delta r_k) = u_k \circ \gamma_k + \left(\frac{\partial u_k}{\partial \mathbf{e}_r} \circ \gamma_k \right) \delta r_k$, we arrive at the update equation

$$(5.2) \quad F(\delta r_k) = u_k \circ \gamma_k + \left[\left(\frac{\partial u_k}{\partial \mathbf{n}} \circ \gamma_k \right) \langle \mathbf{e}_r, \mathbf{n} \rangle + \left(\frac{\partial u_k}{\partial \mathbf{t}} \circ \gamma_k \right) \langle \mathbf{e}_r, \mathbf{t} \rangle \right] \delta r_k \stackrel{!}{=} 0.$$

REMARK 5.1. We mention that the solution of the data completion problem according to Section 4 immediately yields the quantities $u_k|_{\partial\omega_k}$ and $\partial_{\mathbf{n}} u_k|_{\partial\omega_k}$. Since $u_k|_{\partial\omega_k}$ is expressed in terms of trigonometric polynomials, it is also straightforward to compute

$$\left(\frac{\partial u_k}{\partial \mathbf{t}} \circ \gamma_k \right) (s) = \frac{1}{|\gamma_k'(s)|} \frac{\partial u_k}{\partial s} (s).$$

Consequently, all terms required in (5.2) are available.

Since the trial method is fixed-point type iterative method, its convergence is only ensured if it is a contraction. We refer the reader to [42] for sufficient conditions on its convergence.

5.3. Discretization of the sought boundary. For the numerical computations, we discretize the radial function r_k^n associated with the boundary $\partial\omega_k$ by a finite Fourier series according to

$$(5.3) \quad r_k^n(s) = a_0 + \sum_{\ell=1}^{n-1} \{a_\ell \cos(\ell s) + b_\ell \sin(\ell s)\} + a_n \cos(ns).$$

This obviously ensures that r_k^n is always an element of $\mathcal{C}_{\text{per}}([0, 2\pi])$. To determine the update function δr_k^n , represented likewise by a finite Fourier series, we insert the $N \geq 2n$ equidistantly distributed points $s_\ell = 2\pi\ell/N$ into the update equations (5.2):

$$F(\delta r_k^n) \stackrel{!}{=} 0 \quad \text{in all the points } s_1, \dots, s_N.$$

This is a discrete least-squares problem which can simply be solved by the normal equations.

5.4. Numerical results. We shall illustrate our approach by some numerical test examples. We choose Ω as the ball of radius 0.4, which is centered in $\mathbf{0}$. Knowing the inclusion ω , we can compute the current measurements g_m from a given voltage distribution f_m . For the specific voltage distribution $f_m(x, y) = y|_{\partial\Omega}$, we try to reconstruct the inclusion ω in the following by using the synthetic data (f_m, g_m) .

The settings for the data completion algorithm are as in Subsection 4.3, i.e., the regularization parameter ε for the data completion functional (4.1) is set to 0.01, which turned out to be the best choice. We use 200 boundary elements per boundary for the discretization of the boundary integral equations in (4.5) and (4.6), respectively.

The reconstruction is performed by the trial method detailed previously. Precisely, the sought inclusion is represented by a Fourier series with 10 terms, i.e., we have $n = 5$ in (5.3). The initial guess is always a ball of radius 0.3 (always indicated via the red boundary in the subsequent figures) and we stop the trial method after 20 iterations, where the damping factor $h = 0.2$ is used. This means that the update from (5.2) is multiplied with h before computing the new iterate in accordance with (5.1).

In our first example, we consider again the ellipse with semi-axis $h_x = 0.25$ and $h_y = 0.15$ as inclusion ω , compare the left plot of Figure 4.1. In the second example, we have again the potato shaped inclusion ω , compare the right plot of Figure 4.1. We add 1% and 5% noise, respectively, to the respective synthetic current measurement g_m , where noise g_{noise} is generated as a random vector with on $[-1, 1]/\sqrt{n}$ uniformly distributed random variables, such that

$$g_m^\delta := g_m + \delta \|g_m\|_{L^2(\Omega)} g_{\text{noise}}.$$

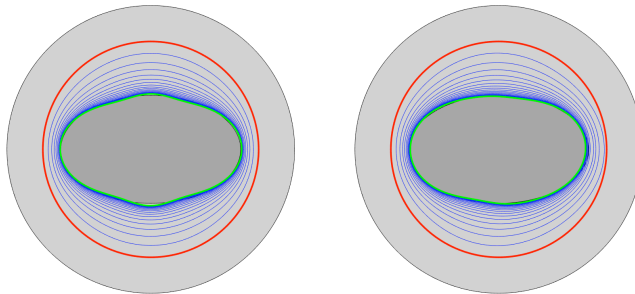


FIG. 5.1. Iterates (in blue) and the final reconstructions (in green) for the ellipse inclusion with 1% noise (left-hand side) and with 5% noise (right-hand side).

The final reconstructions, indicated via the green boundary, can be found in Figure 5.1 for the first example and in Figure 5.2 for the second example; on the left-hand side the reconstructions for the noise level 1% are shown and on the right-hand side the reconstructions for the noise level 5% are shown. The intermediate iterates are indicated by the blue boundaries.

In order to better understand the reconstruction algorithm, we draw 25 realizations with noise level 5% for both obstacles. They can be found in Figure 5.3 for the ellipse inclusion on the left-hand side and for the potato inclusion on the right-hand side. Since we are dealing with starshaped domains, we can compute the mean of the realizations by taking the mean of the respective Fourier coefficients. The mean

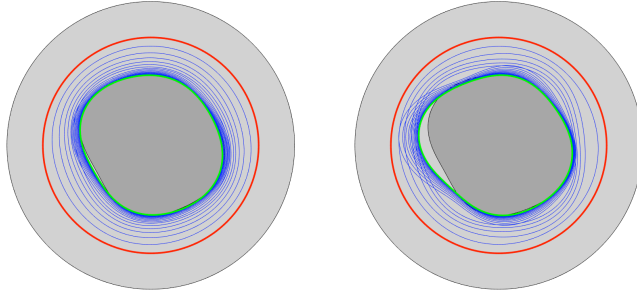


FIG. 5.2. Iterates (in blue) and the final reconstructions (in green) for the potato inclusion with 1% noise (left-hand side) and with 5% noise (right-hand side).

shape is plotted in green. As one readily infers, the reconstructions vary around the mean shapes which basically coincides with the sought inclusions.

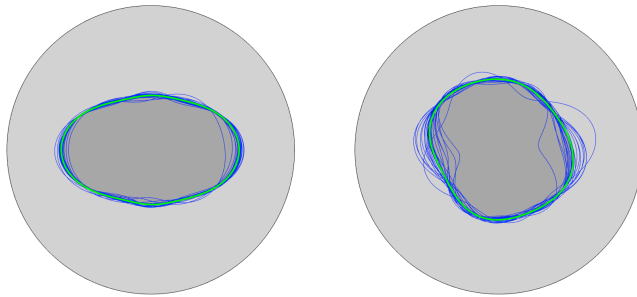


FIG. 5.3. 25 reconstructions and mean shape (in green) in case of the ellipse inclusion (left-hand side) and in case of the potato inclusion (right-hand side).

We shall finally explore the hard case of a non-convex, small obstacle. The results are presented in Figure 5.4. It underlines the fact that the reconstruction is less performant: the right concavity is not perfectly recovered. Moreover, the reconstruction becomes worse when the void becomes smaller.

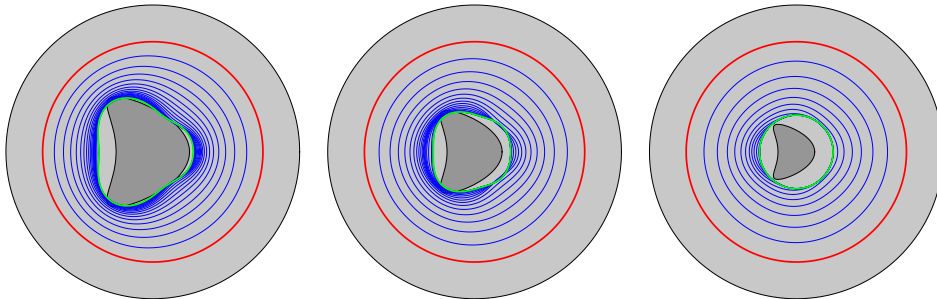


FIG. 5.4. Iterates (in blue) and the final reconstructions (in green) for different scalings of a kite shaped void with 1% noise.

6. Conclusion. In the present article, we solved the data completion problem for Laplace's equation by the minimization of the Kohn-Vogelius functional, which has

been regularized with respect to the associated energy norm. The minimization of the regularized Kohn-Vogelius functional has been performed by a Newton scheme, which results in a direct solver. By employing a collocation method based on trigonometric polynomials, we arrive at a very efficient numerical method for the data completion problem. We then combined this data completion algorithm with the trial method in order to solve an inverse obstacle problem. It updates a given inclusion such that the desired inclusion's homogeneous Dirichlet boundary condition is approximately satisfied. This yields an iterative method for the detection of inclusions in electric impedance tomography.

REFERENCES

- [1] S. Andrieux, T. Baranger, and A.B. Abda. Solving Cauchy problems by minimizing an energy-like functional. *Inverse problems*, 22(1):115, 2006.
- [2] L. Afraites, M. Dambrine, and D. Kateb. Conformal mapping and inverse conductivity problem with one measurement. *ESAIM Control Optim. Calc. Var.*, 13(1):163–177, 2007.
- [3] L. Afraites, M. Dambrine, and D. Kateb. On second order shape optimization methods for electrical impedance tomography. *SIAM J. Control Optim.*, 47(3):1556–1590, 2008.
- [4] G. Alessandrini, E. Beretta, E. Rosset, and S. Vessella. Optimal stability for inverse elliptic boundary value problems with unknown boundaries. *Annali della Scuola Normale Superiore di Pisa - Classe di Scienze*, 29(4):755–806, 2000.
- [5] G. Alessandrini, V. Isakov, and J. Powell. Local uniqueness in the inverse problem with one measurement. *Trans. Am. Math. Soc.*, 347:3031–3041, 1995.
- [6] M. Badra, F. Caubet, and M. Dambrine. Detecting an obstacle immersed in a fluid by shape optimization methods. *Math. Models Methods Appl. Sci.*, 21(10):2069–2101, 2011.
- [7] F. Ben Belgacem and H. El Fekih. On Cauchy's problem: I. A variational Steklov-Poincaré theory. *Inverse Problems*, 21(6):1915, 2005.
- [8] F. Ben Belgacem, H. El Fekih, and F. Jelassi. The Lavrentiev regularization of the data completion problem. *Inverse Problems*, 24(4):045009, 2008.
- [9] A. Beurling. On free-boundary problems for the Laplace equation. *Sem. on analytic functions*, Inst. Adv. Stud. Princeton, 1957, pp. 248–263.
- [10] L. Bourgeois and J. Dardé. A quasi-reversibility approach to solve the inverse obstacle problem. *Inverse Probl. Imaging*, 4(3):351–377, 2010.
- [11] M. Brühl. Explicit characterization of inclusions in electrical impedance tomography. *SIAM J. Math. Anal.*, 32(6):1327–1341, 2001.
- [12] M. Brühl and M. Hanke. Numerical implementation of two noniterative methods for locating inclusions by impedance tomography. *Inverse Problems*, 16(4):1029–1042, 2000.
- [13] F. Caubet, C. Conca, and M. Godoy. On the detection of several obstacles in 2d Stokes flow: topological sensitivity and combination with shape derivatives. *Inverse Problems and Imaging*, 10(2):327–367, 2016.
- [14] F. Caubet, M. Dambrine, and D. Kateb. Shape optimization methods for the inverse obstacle problem with generalized impedance boundary conditions. *Inverse Problems*, 29(11):115011, 26, 2013.
- [15] F. Caubet, M. Dambrine, D. Kateb, and C.Z. Timimoun. A Kohn-Vogelius formulation to detect an obstacle immersed in a fluid. *Inverse Probl. Imaging*, 7(1):123–157, 2013.
- [16] F. Caubet, J. Dardé, and M. Godoy. On the data completion problem and the inverse obstacle problem with partial Cauchy data for Laplace equation. To appear in *ESAIM Control Optim. Calc. Var.*
- [17] R. Chapko and R. Kress. A hybrid method for inverse boundary value problems in potential theory, 2003. *J. Inv. Ill-Posed Problems*, 13(1):27–40, 2005.
- [18] A. Cimetiere, F. Delvare, M. Jaoua, and F. Pons. Solution of the Cauchy problem using iterated Tikhonov regularization. *Inverse Problems*, 17(3):553, 2001.
- [19] D. Colton and R. Kress. *Inverse acoustic and electromagnetic scattering theory*, volume 93 of *Applied Mathematical Sciences*. Springer, Berlin, second edition, 1998.
- [20] M. Di Cristo and L. Rondi. Examples of exponential instability for inverse inclusion and scattering problems. *Inverse Problems*, 19(3):685–701, 2003.
- [21] K. Eppler and H. Harbrecht. A regularized Newton method in electrical impedance tomography using shape Hessian information. *Control Cybernet.*, 34:203–225, 2005.
- [22] M. Flucher and M. Rumpf. Bernoulli's free-boundary problem, qualitative theory and numerical

- approximation. *J. Reine Angew. Math.*, 486:165–204, 1997.
- [23] A. Friedman and V. Isakov. On the uniqueness in the inverse conductivity problem with one measurement. *Indiana Univ. Math. J.*, 38:563–579, 1989.
- [24] A. V. Fursikov. *Optimal control of distributed systems. Theory and applications* American Mathematical Soc., 1999.
- [25] H. Garde and S. Staboulis. Convergence and regularization for monotonicity-based shape reconstruction in electrical impedance tomography *Numer. Math.*, 135 (4):1221–1251, 2017.
- [26] P. Guillaume and K. Sid Idris. Topological sensitivity and shape optimization for the Stokes equations. *SIAM J. Control Optim.*, 43(1):1–31 (electronic), 2004.
- [27] H. Haddar and R. Kress. Conformal mappings and inverse boundary value problems. *Inverse Problems*, 21(3):935–953, 2005.
- [28] B. Harrach and M. Ullrich. Monotonicity-based shape reconstruction in electrical impedance tomography, *SIAM J. Math. Anal.*, 45(6):3382–3403, 2013.
- [29] B. Harrach and E. Lee and M. Ullrich. Combining frequency-difference and ultrasound modulated electrical impedance tomography, *Inverse Problems*, 31(9), 2015.
- [30] M.R. Hestenes and E. Stiefel. Methods of conjugate gradients for solving linear systems. *J. Res. Natl. Stand.*, 49(6):409–436, 1952.
- [31] F. Hettlich and W. Rundell. The determination of a discontinuity in a conductivity from a single boundary measurement. *Inverse Problems*, 14:67–82, 1998.
- [32] R. Kohn and M. Vogelius. Determining conductivity by boundary measurements. *Comm. Pure Appl. Math.*, 37:289–298, 1984.
- [33] V. Kozlov, V. Mazya, and A. Fomin. An iterative method for solving the Cauchy problem for elliptic equations. *Zhurnal Vychislitelnoi Matematiki i Matematicheskoi Fiziki*, 31(1):6474, 1991.
- [34] R. Kress. *Linear integral equations*. Vol. 82 of Applied Mathematical Sciences, Springer, New York, 2nd ed., 1999.
- [35] R. Kress and W. Rundell. Nonlinear integral equations and the iterative solution for an inverse boundary value problem. *Inverse Problems*, 21(4):1207–1223, 2005.
- [36] A. Lechleiter, N. Hyvönen and H. Hakula. The factorization method applied to the complete electrode model of impedance tomography *SIAM J. Appl. Math.*, 68(4):1097–1121, 2008.
- [37] W. Lionheart, N. Polydorides, and A. Borsic. Electrical Impedance Tomography: Methods, History and Applications. In D.S. Holder, editor, *IOP Series in Medical Physics and Biomedical Engineering*, pages 3–64, Institute of Physics Publishing, 2005.
- [38] R. Potthast. A survey on sampling and probe methods for inverse problems. *Inverse Problems*, 22(2):R1–R47, 2006.
- [39] J.-R. Roche and J. Sokolowski. Numerical methods for shape identification problems. *Control Cybern.* 25:867–894, 1996.
- [40] W. Rundell. Recovering an obstacle using integral equations. *Inverse Probl. Imaging*, 3(2):319–332, 2009.
- [41] P. Serranho. A hybrid method for inverse obstacle scattering problems. PhD thesis, Georg-August-Universität Göttingen, 2007.
- [42] T. Tiihonen and J. Järvinen. On fixed point (trial) methods for free boundary problems. In *Free Boundary Problems in Continuum Mechanics (Novosibirsk, 1991)*. Vol. 106 of Internat. Ser. Numer. Math., Birkhäuser, Basel, 1992, pp. 339–350.